Appendix 1 to Stephenson, D, El Shaikh, A, Shaff, N et al. Differing Functional Mechanisms Underlie Cognitive Control Deficits in Psychotic Spectrum Disorders. *J Psychiatry Neurosci* 2020.

DOI: 10.1503/jpn.190212

Online appendices are unedited and posted as supplied by the authors.

Supplemental Materials

Participant Information

One hundred fifty-four patients diagnosed with a psychotic spectrum disorder (PSD; 96 males, 32.00±9.28 years old) were consecutively recruited in this Research Domain Criteria (RDoC) study.[1] Patients, recruited from local psychiatric centers and newspaper ads, were diagnosed with a psychotic spectrum disorder by a board-certified psychiatrist using the Structured Clinical Interview for DSM-IV-TR (SCID-II).[2] A total of 65 healthy controls (HC) (41 males, 33.25±8.15 years old) were recruited from the local community through informal oral correspondence and public fliers.

Clinical and Neuropsychological Assessments

All participants completed the Wechsler Test of Adult Reading (WTAR),[3] the Measurement and Treatment Research to Improve Cognition in Schizophrenia Consensus Cognitive Battery (MCCB),[4] the Executive Abilities: Measures and Instruments for Neurobehavioral Evaluation and Research (EXAMINER),[5] the Edinburgh Handedness Inventory (EHI),[6] a 60-day Timeline Followback (TLFB),[7] and a medical history form and the Fagerstrom Test for Nicotine Dependence (FTND).[8] Everyday functioning was assessed with the UCSD Performance-Based Skills Assessment Brief Version (UPSA-B)[9] and the Quality of Life Questionnaire in Schizophrenia 18 (S-QoL 18).[10] All participants also completed a form detailing recent caffeine intake, cigarette consumption, alcohol consumption and sleep for the 24 hours prior to scan. Participants were asked to refrain from smoking for at least one hour prior to their appointment and CO levels were monitored with a Vitolograph BreathCO Monitor for all smokers.

PSD completed additional clinical instruments, which included the Positive and Negative Syndrome Scale (PANSS),[11] Schizo-Bipolar Scale (SBS)[12] and Clinical Global Impressions Scale (CGI).[13] Extrapyramidal symptoms were assessed with the Abnormal Involuntary Movement Scale (AIMS),[14] Barnes Akathisia Scale (BAS)[15] and a modified Simpson Angus Scale (SAS).[16] PSD family members were also contacted whenever available to complete a modified version of the Specific Levels of Functioning Informant Scale (SLOF-I).[17] Finally, an olanzapine equivalence metric was calculated for all patients to determine medication load.[18]

AX-CPT Practice Parameters

Prior to entering the scanner, participants received active instructions with examples of cue-probe conditions and expected target/non-target responses. This was followed by up to three blocks of practice trials for the task. Practice consisted of maximum trial counts of AX=9, AY=12, BX=6, BY=3. Note that this proportion of conditions (AX=30%; AY=40%; BX=20%; BY=10%) was intentionally different from the standard AX-CPT proportions, ensuring that participants were exposed to enough non-target conditions to ensure that they understood the task while minimizing overtraining. All participants were eventually scanned regardless of performance following RDoC conventions.[1]

Appendix 1 to Stephenson, D, El Shaikh, A, Shaff, N et al. Differing Functional Mechanisms Underlie Cognitive Control Deficits in Psychotic Spectrum Disorders. *J Psychiatry Neurosci* 2020.

DOI: 10.1503/jpn.190212

Online appendices are unedited and posted as supplied by the authors.

Imaging Protocol and Preprocessing

High resolution 5-echo multi-echo Magnetization Prepared Rapid Acquisition Gradient Echo (MPRAGE) T_1 [repetition time (TR)=2530ms; echo times (TE)=1.64, 3.5, 5.36, 7.22, 9.08ms; inversion time (TI)=1200ms; flip angle=7°; number of excitations (NEX)=1; slice thickness=1mm; field of view (FOV)=256mm; matrix size=256×256; isotropic voxels=1mm] were collected for structural images on a 3T Siemens Trio Tim scanner. Echo-planar images were collected for four runs of the AX-CPT task using a single-shot, gradient-echo echoplanar pulse sequence with simultaneous multi-slice technology [TR=460ms; TE=29ms; flip angle=44°; multiband acceleration factor=8; NEX=1; slice thickness=3mm; FOV=248mm; matrix size=82×82; 56 interleaved slices; 3.02×3.02×3.00mm voxels]. The first three images of each run were eliminated to account for T_1 equilibrium effects, resulting in 3116 images in final analysis of the AX-CPT. A single band reference image (SBREF) was also acquired to facilitate registration with the T_1 image. Two EPI distortion mapping pre-scan sequences [TR=7220ms; TE=73ms; flip angle=90°; refocus flip angle=180°; slice thickness=3 mm; FOV=248mm; matrix size=82×82; 56 interleaved slices; 3.02×3.02×3.00mm voxels] with reversed phase encoding directions (A → P; P → A) were also collected to correct for susceptibility related artifacts in the task data.

Anomalous time-series data were first identified and replaced based on values from the previous and subsequent image using AFNI's despiking protocol.[19] All time-series data were then temporally interpolated to the first slice for slice acquisition differences, spatially registered in two- and three-dimensional space to the EPI reference image to reduce the effects of head motion. Mean frame-wise displacement (FD) was calculated across 3 rotational motion parameters and 3 displacement parameters.[20] Susceptibility field distortion was estimated and corrected using FSL Topup.[21,22] Task data were converted to standard stereotaxic coordinate space[23] using a non-linear algorithm (AFNI 3dQwarp) and spatially blurred (6-mm Gaussian FWHM filter). A voxel-wise deconvolution analysis generated a single hemodynamic response function for each trial-type relative to the baseline state (visual fixation plus gradient noise) based on the first 14.26 seconds post-stimulus onset.[24] Error trials were modelled separately for each trial-type to eliminate error variance.[25]

Behavioral Index Measures

To test within-group equality of variance across specified contrasts, Pitman-Morgan tests were used to generate a correlation coefficient between the sum (e.g., Cue A + Cue B) and difference (e.g., Cue A – Cue B) across conditions.[26] The correlation term was then transformed using Fisher's r-to-z to assess between group differences.[27,28] The d'-index was calculated [*z*(AX-Hits) – *z*(BX-False Alarms)] to determine participants contextual sensitivity to cue information influencing responses to the probe,[29-31] while the behavioral shift index (BSI; AY-BX/AY+BX) was calculated to determine if a proactive (BSI > 0) or reactive (BSI < 0) cognitive control strategy was being employed during specific conditions (Supplemental Table 1).[30,32]

Appendix 1 to Stephenson, D, El Shaikh, A, Shaff, N et al. Differing Functional Mechanisms Underlie Cognitive Control Deficits in Psychotic Spectrum Disorders. *J Psychiatry Neurosci* 2020.

DOI: 10.1503/jpn.190212

Online appendices are unedited and posted as supplied by the authors.

Simulation of delayed Hemodynamic response functions (HRF)

Simulations with HRFs were performed in AFNI[19] to assess the effect of delayed hemodynamic activity on estimated group differences. Event timing was based on the pseudorandom presentation of AX probes, and AFNI's 3dDeconvolve was used to model expected neural response with a double gamma variate function. In addition to this unshifted function, a family of offsets (every 460 ms [1 TR] between 460-4,600) was applied to create delayed neural response files. Realistic noise was generated for all unshifted and shifted simulated data separately using AFNI's 1dgenARMA11, which models noise with an autoregressive moving average model (ARMA). The standard deviation (SD=0.3) of the noise model was selected to mimic what would be commonly seen for average neural response in the sensorimotor cortex (see Figure 3B). After noise addition, 3dfim+ was used to determine the β coefficient of each simulated signal to the ideal double gamma response function. This process was repeated 100 times, modeling noise separately for all repetitions. Next, jackknife resampling (1000 permutations) across samples of 20 to 100 was performed to indicate the percentage of significant differences between β coefficients for the unshifted and shifted data with $p < 0.001$ to mirror the latest recommendations for false positive correction on a voxel-wise level.[33]

Results

Behavioral Results.

To more effectively model the hemodynamic response function, only those participants with ≥ 56% accuracy across all trials were included in principal analyses. However, to maintain consistency with previous behavioral investigations of AX-CPT patterns in SZ/PSD,[34-36] the principal reaction time (RT) analyses (Condition: Cue [A vs. B], Probe [AY vs. BX], Cue vs. Probe [A vs. AY; B vs. BX]) were repeated using good and poor performers (PSD_{all}) and the same 2×2 (Group: HC vs. PSD_{all} × Condition) repeated measure ANOVAs. Similar to previous findings, a main effect of Group (PSD_{all} > HC) was present in all four ANOVAs (all p's<0.05). However, the Condition×Group interaction was also significant in the AY vs. BX analysis ($F_{1,205}$=9.17, p=0.003). Follow-up tests indicated a greater difference between AY and BX trials for the HC ($F_{1,205}$=33.60, $p \leq 0.001$) compared to PSD_{all} ($F_{1,205}$=12.31, $p \leq 0.001$) group. Similar to previous findings,[34-36] these findings indicate a greater deficit in proactive compared to reactive cognitive control in the PSD_{all} group. However, it is also critical to recognize that this finding was primarily driven by PSD_{pp} (Supplemental Table 2 and Supplemental Figure 1), and that performance accuracy was too low to permit adequate modeling of the hemodynamic response.

Differences in covariance between groups were assessed through Pitman-Morgan tests within the contrast assessing proactive cognitive control (AY vs. BX). Both HC (t_{57}=-5.66; p<0.001) and good performing PSD (PSD_{gp}; t_{106}=-6.17; p<0.001) demonstrated similar covariance differences, with greater variance for BX relative to AY conditions. Accordingly, no difference in covariance magnitude between groups was observed (Z=-0.66; p=0.51).

Appendix 1 to Stephenson, D, El Shaikh, A, Shaff, N et al. Differing Functional Mechanisms Underlie Cognitive Control Deficits in Psychotic Spectrum Disorders. *J Psychiatry Neurosci* 2020.

DOI: 10.1503/jpn.190212

Online appendices are unedited and posted as supplied by the authors.

The multimodal nature of the AX-CPT may have produced sensory confounds in working memory processing. However, results from our previous study in HC[24] produced behavioral performance patterns similar to studies using the unimodal version of the AX-CPT in HC,[32,37] and performance values of the full PSD cohort (Supplemental Table 3) using common AX-CPT clinical threshold criteria (i.e., error rate greater than or equal to 56% on AX, 100% on AY or BX, or 50% on BY)[38] was within range of unimodal AX-CPT performance in SZ[34,35,39,40] and BP-I,[41] suggesting that cognitive control functions in a supramodal fashion.

Condition Effects and Condition×Time Interaction Effects

A series of 2×2×2 [Group (PSD vs. HC)×Condition×Time (Peak vs. Late-peak)] mixed-measures ANCOVAs, with mean FD as a covariate, examined functional activation across the principal contrasts, with Condition effects and Condition×Time interactions explored here. The cue (A vs. B) contrast demonstrated a Condition main effect for the bilateral dorsolateral prefrontal cortex (DLPFC; $F_{1,159}$=7.11, p=0.008; partial η^2=0.04) and ventrolateral prefrontal cortex (VLPFC; $F_{1,160}$=4.70, p=0.032; partial η^2=0.03), with both ROIs demonstrating increased activity for B relative to A cues. The probe (AY vs. BX) contrast exhibited a Condition×Time interaction ($F_{1,160}$=5.84, p=0.017; partial η^2=0.04) only within the VLPFC, with both conditions evidencing a Time pattern of Peak>Late-peak activity, albeit a greater magnitude of difference for AY relative to BX (p=0.007) conditions. For the A vs. AY contrast, results indicated a Condition×Time interaction ($F_{1,158}$=4.28, p=0.040; partial η^2=0.03) and Condition effect ($F_{1,158}$=7.77, p=0.006; partial η^2=0.05) in the DLPFC, with greater activity in the AY relative to A condition, and both conditions demonstrating significant Peak>Late-peak activity for Time, with the A cue showing a greater magnitude of Peak change (p<0.001) than the AY (p=0.002) probe. For VLPFC activity, there was an effect of Condition only ($F_{1,160}$=18.98, p<0.001; partial η^2=0.11), indicating greater overall activity in the AY relative to A condition. The B vs. BX contrast did not demonstrate any Condition effects or Condition×Time interactions for either DLPFC or VLPFC (all p's>0.05).

Whole Brain Results

Assessing whole brain activity for the cue (A vs. B) contrast, a Condition×Time interaction was observed in the anterior (aDMN) and posterior (pDMN) default mode network, with significant deactivation in the Late-peak phase during B relative to A conditions (Supplemental Figure 3A&B), as was previously observed[24] within HC. There was also a Condition main effect of Cue (B>A) in the right anterior insula/VLPFC (aINS/VLPFC), bilateral DLPFC and supplemental motor area (SMA), bilateral posterior parietal cortex (PPC), left inferior temporal gyrus (ITG), and left Lobule VI of the cerebellum (Supplemental Figure 3A & 3C).

For the probe (AY vs. BX) contrast, there were Condition×Time interactions following two general patterns of activation (Supplemental Figure 4A). The bilateral inferior parietal lobule (IPL), left superior temporal gyrus (STG), right caudate/putamen, left lentiform nucleus, and left

Appendix 1 to Stephenson, D, El Shaikh, A, Shaff, N et al. Differing Functional Mechanisms Underlie Cognitive Control Deficits in Psychotic Spectrum Disorders. *J Psychiatry Neurosci* 2020.

DOI: 10.1503/jpn.190212

Online appendices are unedited and posted as supplied by the authors.

Lobule VIIa/VIIb of the cerebellum exhibited decreased activation during Peak relative to Late-peak phases during AY, but not BX trials. Both the left temporal pole and left parahippocampal gyrus (PHG) displayed no difference between AY and BX trials during the Peak phase, but differences between probe trials (temporal pole: LP>0>P; PHG: P>0>LP) during the Late-peak phase. Finally, there was a Condition main effect of Probe for the bilateral superior temporal gyrus (STG; extending to MTG on right), demonstrating overall elevated activity for AY relative to BX conditions.

For the B vs. BX contrast, there were Condition×Time interactions demonstrating a number of patterns (Supplemental Figure 4B). Both the bilateral aINS and bilateral auditory cortex (A1) exhibited no difference between Peak and Late-peak for B cues. However, for BX probes, A1 showed greater Peak than Late-peak activation, while the aINS showed greater Late-peak than Peak activation. Conversely, the anterior cingulate cortex (ACC) and dorsomedial PFC demonstrated greater deactivation from Peak to Late-peak in B cues as well as increased activity from Peak to Late-peak in BX probes. The bilateral ventral visual streams showed greater Peak than Late-peak activation in B cues only, whereas the right dorsal visual stream showed greater activation during the Peak, but not Late-peak, phase for B relative to BX trials. There was no unique activation as part of the main effect of Condition.

For the A vs. AY contrast, there was widespread significant Condition×Time interaction throughout the brain (Supplemental Figure 4C). Generally, this resulted from increased activation during Late-peak relative to Peak phases in A cues but not AY probes. However, the STG showed increased activity for Peak relative to Late-peak phases during A cues, with little activity during AY probes, while the anterior vermis exhibited a greater magnitude of activation difference between Peak and Late-peak phases for A cues relative to AY probes. Areas exhibiting a main effect of Condition in this analysis were largely consistent with the interaction, with the addition of the anterior PFC and pre-SMA. Here, the anterior PFC demonstrated deactivation in A cues and activation in AY probes, whereas the pre-SMA activated during A cues but not AY probes.

References

1. Insel T, Cuthbert B, Garvey M, et al. Research domain criteria (RDoC): toward a new classification framework for research on mental disorders. *Am J Psychiatry*. 2010;167(7):748-51.

Appendix 1 to Stephenson, D, El Shaikh, A, Shaff, N et al. Differing Functional Mechanisms Underlie Cognitive Control Deficits in Psychotic Spectrum Disorders. *J Psychiatry Neurosci* 2020.

DOI: 10.1503/jpn.190212

Online appendices are unedited and posted as supplied by the authors.

2. First MB, Spitzer RL, Gibbon M, Williams JB. *Structured Clinical Interview for DSM-IV Axis I Disorders (SCID-I), Clinician Version, Administration Booklet*. Arlington, VA: American Psychiatric Pub; 2012.

3. Wechsler D. *Wechsler Test of Adult Reading: WTAR*. New York, NY: Psychological Corporation; 2001.

4. Kern RS, Green MF, Nuechterlein KH, et al. NIMH-MATRICS survey on assessment of neurocognition in schizophrenia. *Schizophr Res.* 2004;72(1):11-9.

5. Kramer JH, Mungas D, Possin KL, et al. NIH EXAMINER: conceptualization and development of an executive function battery. *J Int Neuropsychol Soc.* 2014;20(1):11-9.

6. Oldfield RC. The assessment and analysis of handedness: the Edinburgh inventory. *Cognitive Neuropsychology.* 1971;9(1):97-113.

7. Sobell LC, Sobell MB. Timeline followback user's guide: A calendar method for assessing alcohol and drug use. *Toronto: Addiction Research Foundation.* 1996.

8. Heatherton TF, Kozlowski LT, Frecker RC, et al. The Fagerstrom Test for Nicotine Dependence: a revision of the Fagerstrom Tolerance Questionnaire. *Br J Addict.* 1991;86(9):1119-27.

9. Patterson TL, Goldman S, McKibbin CL, et al. UCSD Performance-Based Skills Assessment: development of a new measure of everyday functioning for severely mentally ill adults. *Schizophr Bull.* 2001;27(2):235-45.

10. Boyer L, Simeoni MC, Loundou A, et al. The development of the S-QoL 18: a shortened quality of life questionnaire for patients with schizophrenia. *Schizophr Res.* 2010;121(1-3):241-50.

11. Kay SR, Fiszbein A, Opler LA. The Positive and Negative Syndrome Scale (PANSS) for schizophrenia. *Schizophrenia Bull.* 1987;13(2):261-76.

12. Keshavan MS, Morris DW, Sweeney JA, et al. A dimensional approach to the psychosis spectrum between bipolar disorder and schizophrenia: the Schizo-Bipolar Scale. *Schizophr Res.* 2011;133(1-3):250-4.

Appendix 1 to Stephenson, D, El Shaikh, A, Shaff, N et al. Differing Functional Mechanisms Underlie Cognitive Control Deficits in Psychotic Spectrum Disorders. *J Psychiatry Neurosci* 2020.

DOI: 10.1503/jpn.190212

Online appendices are unedited and posted as supplied by the authors.

13. Guy W. Clinical global impression scale. *ECDEU assessment manual for psychopharmacology.* 1976;338:218-22.

14. Guy W. Abnormal involuntary movement scale (AIMS). *ECDEU assessment manual for psychopharmacology.* 1976;338:534-7.

15. Barnes TR. A rating scale for drug-induced akathisia. *Br J Psychiatry.* 1989;154:672-6.

16. Simpson GM, Angus JW. A rating scale for extrapyramidal side effects. *Acta Psychiatr Scand Suppl.* 1970;212:11-9.

17. Schneider LC, Struening EL. SLOF: a behavioral rating scale for assessing the mentally ill. *Soc Work Res Abstr.* 1983;19(3):9-21.

18. Gardner DM, Murphy AL, O'Donnell H, et al. International consensus study of antipsychotic dosing. *Am J Psychiatry.* 2010;167(6):686-93.

19. Cox RW. AFNI: Software for analysis and visualization of functional magnetic resonance neuroimages. *Comput Biomed Res.* 1996;29:162-73.

20. Power JD, Barnes KA, Snyder AZ, et al. Spurious but systematic correlations in functional connectivity MRI networks arise from subject motion. *Neuroimage.* 2012;59(3):2142-54.

21. Andersson JL, Skare S, Ashburner J. How to correct susceptibility distortions in spin-echo echo-planar images: application to diffusion tensor imaging. *Neuroimage.* 2003;20(2):870-88.

22. Smith SM, Jenkinson M, Woolrich MW, et al. Advances in functional and structural MR image analysis and implementation as FSL. *Neuroimage.* 2004;23 Suppl 1:S208-S219.

23. Talairach J,.Tournoux P. *Co-planar stereotaxic atlas of the human brain*. New York: Thieme; 1988.

24. Ryman SG, El Shaikh AA, Shaff NA, et al. Proactive and reactive cognitive control rely on flexible use of the ventrolateral prefrontal cortex. *Hum Brain Mapp.* 2018.

25. Mayer AR, Teshiba TM, Franco AR, et al. Modeling conflict and error in the medial frontal cortex. *Hum Brain Mapp.* 2012;33(12):2843-55.

Appendix 1 to Stephenson, D, El Shaikh, A, Shaff, N et al. Differing Functional Mechanisms Underlie Cognitive Control Deficits in Psychotic Spectrum Disorders. *J Psychiatry Neurosci* 2020.

DOI: 10.1503/jpn.190212

Online appendices are unedited and posted as supplied by the authors.

26. Piepho HP. Tests for equality of dispersion in divariate samples-review and empirical comparison. *Journal of Statistical Computation and Simulation.* 1997;56(4):353-72.

27. Field A, Miles J, Field Z. *Discovering statistics using R*. Sage; 2012.

28. Howell DC. *Statistical methods for psychology*. Cengage; 2010.

29. Barch DM, Carter CS, Braver TS, et al. Selective deficits in prefrontal cortex function in medication-naive patients with schizophrenia. *Arch Gen Psychiatry.* 2001;58(3):280-8.

30. Gonthier C, Macnamara BN, Chow M, et al. Inducing Proactive Control Shifts in the AX-CPT. *Front Psychol.* 2016;7:1822.

31. Stanislaw H, Todorov N. Calculation of signal detection theory measures. *Behav Res Methods Instrum Comput.* 1999;31(1):137-49.

32. Braver TS, Paxton JL, Locke HS, et al. Flexible neural mechanisms of cognitive control within human prefrontal cortex. *Proc Natl Acad Sci U S A.* 2009;106(18):7351-6.

33. Eklund A, Nichols TE, Knutsson H. Cluster failure: Why fMRI inferences for spatial extent have inflated false-positive rates. *Proc Natl Acad Sci U S A.* 2016;113(28):7900-5.

34. Edwards BG, Barch DM, Braver TS. Improving prefrontal cortex function in schizophrenia through focused training of cognitive control. *Front Hum Neurosci.* 2010;4:32.

35. Lesh TA, Westphal AJ, Niendam TA, et al. Proactive and reactive cognitive control and dorsolateral prefrontal cortex dysfunction in first episode schizophrenia. *Neuroimage Clin.* 2013;2:590-9.

36. Niendam TA, Lesh TA, Yoon J, et al. Impaired context processing as a potential marker of psychosis risk state. *Psychiatry Res.* 2014;221(1):13-20.

37. Paxton JL, Barch DM, Racine CA, et al. Cognitive control, goal maintenance, and prefrontal function in healthy aging. *Cereb Cortex.* 2008;18(5):1010-28.

38. Henderson D, Poppe AB, Barch DM, et al. Optimization of a goal maintenance task for use in clinical applications. *Schizophr Bull.* 2012;38(1):104-13.

Appendix 1 to Stephenson, D, El Shaikh, A, Shaff, N et al. Differing Functional Mechanisms Underlie Cognitive Control Deficits in Psychotic Spectrum Disorders. *J Psychiatry Neurosci* 2020.

DOI: 10.1503/jpn.190212

Online appendices are unedited and posted as supplied by the authors.

39. Barch DM, Carter CS, MacDonald AW, III, et al. Context-processing deficits in schizophrenia: diagnostic specificity, 4-week course, and relationships to clinical symptoms. *J Abnorm Psychol.* 2003;112(1):132-43.

40. Poppe AB, Barch DM, Carter CS, et al. Reduced Frontoparietal Activity in Schizophrenia Is Linked to a Specific Deficit in Goal Maintenance: A Multisite Functional Imaging Study. *Schizophr Bull.* 2016;42(5):1149-57.

41. Smucny J, Lesh TA, Newton K, et al. Levels of Cognitive Control: A Functional Magnetic Resonance Imaging-Based Test of an RDoC Domain Across Bipolar Disorder and Schizophrenia. *Neuropsychopharmacology.* 2018;43(3):598-606.

42. Carter CS, Braver TS, Barch DM, et al. Anterior cingulate cortex, error detection, and the online monitoring of performance. *Psychobiology.* 1998;280(5364):747-9.

43. Carter CS, MacDonald AW, III, Ross LL, et al. Anterior cingulate cortex activity and impaired self-monitoring of performance in patients with schizophrenia: an event-related fMRI study *Am J Psychiatry.* 2001;158(9):1423-8.

44. MacDonald AW, Cohen JD, Stenger VA, et al. Dissociating the role of the dorsolateral prefrontal and anterior cingulate cortex in cognitive control. *Psychobiology.* 2003;288(5472):1835-8.

45. Locke HS, Braver TS. Motivational influences on cognitive control: behavior, brain activation, and individual differences. *Cogn Affect Behav Neurosci.* 2008;8(1):99-112.

46. Yoon JH, Minzenberg MJ, Ursu S, et al. Association of dorsolateral prefrontal cortex dysfunction with disrupted coordinated brain activity in schizophrenia: relationship with impaired cognition, behavioral disorganization, and global function. *Am J Psychiatry.* 2008;165(8):1006-14.

47. Yoon JH, Nguyen DV, McVay LM, et al. Automated classification of fMRI during cognitive control identifies more severely disorganized subjects with schizophrenia. *Schizophr Res.* 2012;135(1-3):28-33.

48. Lesh TA, Tanase C, Geib BR, et al. A multimodal analysis of antipsychotic effects on brain structure and function in first-episode schizophrenia. *JAMA Psychiatry.* 2015;72(3):226-34.

Appendix 1 to Stephenson, D, El Shaikh, A, Shaff, N et al. Differing Functional Mechanisms Underlie Cognitive Control Deficits in Psychotic Spectrum Disorders. *J Psychiatry Neurosci* 2020.

DOI: 10.1503/jpn.190212

Online appendices are unedited and posted as supplied by the authors.

49. Lopez-Garcia P, Lesh TA, Salo T, et al. The neural circuitry supporting goal maintenance during cognitive control: a comparison of expectancy AX-CPT and dot probe expectancy paradigms. *Cogn Affect Behav Neurosci.* 2016;16(1):164-75.

50. Niendam TA, Ray KL, Iosif AM, et al. Association of Age at Onset and Longitudinal Course of Prefrontal Function in Youth With Schizophrenia. *JAMA Psychiatry.* 2018;75(12):1252-60.

51. Ryman SG, Cavanagh JF, Wertz CJ, et al. Impaired Midline Theta Power and Connectivity During Proactive Cognitive Control in Schizophrenia. *Biol Psychiatry.* 2018;84(9):675-83.

Appendix 1 to Stephenson, D, El Shaikh, A, Shaff, N et al. Differing Functional Mechanisms Underlie Cognitive Control Deficits in Psychotic Spectrum Disorders. *J Psychiatry Neurosci* 2020.

DOI: 10.1503/jpn.190212

Online appendices are unedited and posted as supplied by the authors.

Supplemental Table 1: Literature review of fMRI AX-CPT studies and contrasts employed.

Author	Year	Behavioral Contrasts	Imaging Contrast	Cognitive Measure
Carter et al.[42]	1998	*NA*	All Probes	Error/Competition
Barch et al.[29]	2001	d'-index; RT and ACC ANOVAs (Group x Trial x Delay)	Delay (Long vs. Short)	Context Maintenance
Carter et al.[43]	2001	RT Correct vs Incorrect Responses (collapsed across all probes)	Correct vs Incorrect Trials (across all probes)	Error Monitoring
MacDonald et al.[44]	2003	Accuracy for all probes, d'-index, AY & BX interference scores	Cue (B-A)	Context Processing
Locke & Braver[45]	2008	ANOVA (Condition); all probes	AX condition (assessing reward manipulation)	Proactive/Reactive
Paxton et al.[37]	2008	ANOVA (Probe x Group); all probes	Cue vs Probe; BX vs Baseline; BX vs. BY	Goal Maintenance
Yoon et al.[46]	2008	ANOVA (Probe x Group); all probes	Cue (B-A)	High/Low Control
Braver et al.[32]	2009	NA	Cue vs Probe	Proactive/Reactive
Edwards et al.[34]	2010	AY vs. BX	Cue (B-A); Cue vs Probe	Proactive/Reactive
Yoon et al.[47]	2012	AX vs. BX	Cue (B-A)	High/Low Control
Lesh et al.[35]	2013	ANOVA (Probe x Group); all probes	Cue (B-A)	Proactive/Reactive
Niendam et al.[36]	2014	ANOVA (Probe x Group); all probes	Cue (B-A)	High/Low Control
Poppe et al.[40]€	2016	d'-index & accuracy for all probes	Cue (B-A)	Goal Maintenance
Lesh et al.[48]‡	2015	ANOVA with d-prime index	Cue (B-A)	High/Low Control
Lopez-Garcia et al.[49]	2015	Cue vs Probe	Cue (B-A)	Goal Maintenance
Niendam et al.[50]	2018	Analyzed d'- index	Cue (B-A)	High/Low Control
Ryman et al.[51]¥	2018	ANOVA (Condition x Group): A vs. B; AX vs. AY; AX vs. BX	A vs. B; AX vs. AY; AX vs. BX	Proactive/Reactive
Ryman et al.[24]	2018	t-test: AX vs. AY vs. BX conditions	A vs. B; AX vs. AY; AX vs. BX; AY vs. BX	Proactive/Reactive
Smucny et al.[41]	2018	d'-index	Cue (B-A)	High/Low Control

NOTE: € = DPX variant of AX-CPT; ¥ = EEG study.

Appendix 1 to Stephenson, D, El Shaikh, A, Shaff, N et al. Differing Functional Mechanisms Underlie Cognitive Control Deficits in Psychotic Spectrum Disorders. *J Psychiatry Neurosci* 2020.

DOI: 10.1503/jpn.190212

Online appendices are unedited and posted as supplied by the authors.

Supplemental Table 2: Reaction Time Data Across Groups for AX-CPT

AX-CPT RT	HC (N=59)	PSD_{gp} (N=108)	PSD_{pp} (N=46)
A_{cue}	620.46±179.79	719.83±173.68	888.06±285.65†
B_{cue}	677.41±166.91	756.63±165.72	915.80±206.17†
AX	627.66±133.32	680.12±156.09	837.47±252.25†
AY	832.30±156.31	906.05±176.86	979.69±180.93†
BX	653.51±271.41	785.92±281.38	1018.65±328.32†
BY	698.11±197.11	806.91±206.13	1027.73±234.71†

RT: reaction time (ms); HC: Healthy Controls; PSD_{gp}: Psychotic Spectrum Disorder- Good Performers; PSD_{pp}: Psychotic Spectrum Disorder- Poor Performers; e*ff*: Cohen's d effect size; AB: HC vs. PSD_{gp}; BC: PSD_{gp} vs. PSD_{pp}; AC: HC vs. PSD_{pp}; NA: Not Applicable since not a principal analyses/condition; †: Variable N due to exclusions of participants with complete of near complete inaccuracy (A_{cue}=41; B_{cue}=44; AX=43; AY=43; BX=41; BY=40).

Appendix 1 to Stephenson, D, El Shaikh, A, Shaff, N et al. Differing Functional Mechanisms Underlie Cognitive Control Deficits in Psychotic Spectrum Disorders. *J Psychiatry Neurosci* 2020.

DOI: 10.1503/jpn.190212

Online appendices are unedited and posted as supplied by the authors.

Supplemental Table 3: Performance parameters for AX-CPT after common threshold exclusions†

Accuracy	HC (n=64)	SP (n=88)	SCA (n=11)	BPD-I (n=36)
AX	0.95±0.08	0.88±0.13	0.92±0.08	0.93±0.08
AY	0.94±0.09	0.91±0.09	0.90±0.09	0.93±0.09
BX	0.90±0.17	0.77±0.24	0.79±0.22	0.87±0.14
BY	0.97±0.07	0.91±0.12	0.97±0.03	0.95±0.08
RT				
AX	635.89±134.46	723.10±185.58	715.20±121.08	656.26±128.59
AY	839.19±156.29	922.21±173.57	955.53±163.38	894.66±180.81
BX	676.24±275.65	870.15±350.29	931.57±236.58	731.17±269.50
BY	711.21±199.56	866.98±237.98	849.82±119.78	782.26±189.11

HC=healthy control; SP= Schizophrenia; SCA= Schizoaffective; BP-I= Bipolar Disorder Type I; Reported values are mean and standard deviation. †=Threshold of performance parameters based on common criteria for clinical AX-CPT[38], which indicates similar parameters relative to unimodal applications of the AX-CPT.

Appendix 1 to Stephenson, D, El Shaikh, A, Shaff, N et al. Differing Functional Mechanisms Underlie Cognitive Control Deficits in Psychotic Spectrum Disorders. *J Psychiatry Neurosci* 2020.

DOI: 10.1503/jpn.190212

Online appendices are unedited and posted as supplied by the authors.

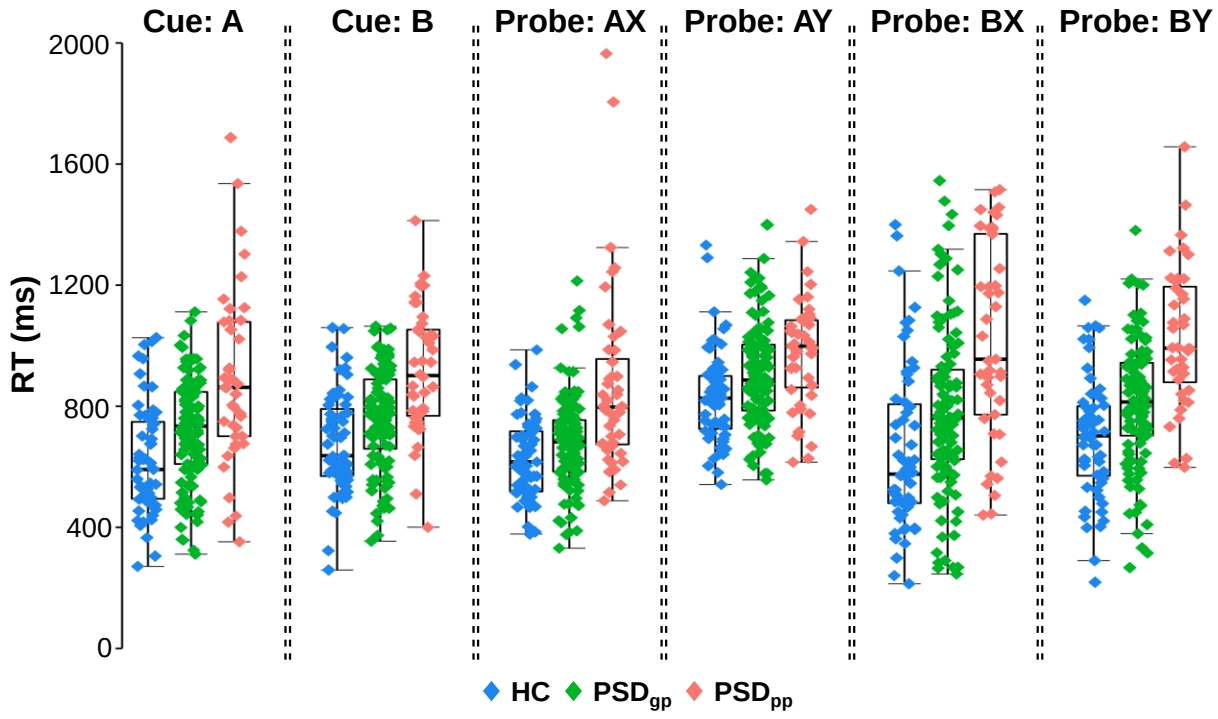

Supplemental Figure 1: Box-and-scatter plots depict reaction times (RT) between healthy controls (HC; N=58; blue diamonds), good-performing (≥56% accuracy on all conditions) patients with psychotic spectrum disorder (PSD_{gp}; N=105; green diamonds), and poor-performing (<56% accuracy on any condition) PSD (PSD_{pp}; N=46; salmon diamonds).

Appendix 1 to Stephenson, D, El Shaikh, A, Shaff, N et al. Differing Functional Mechanisms Underlie Cognitive Control Deficits in Psychotic Spectrum Disorders. *J Psychiatry Neurosci* 2020.

DOI: 10.1503/jpn.190212

Online appendices are unedited and posted as supplied by the authors.

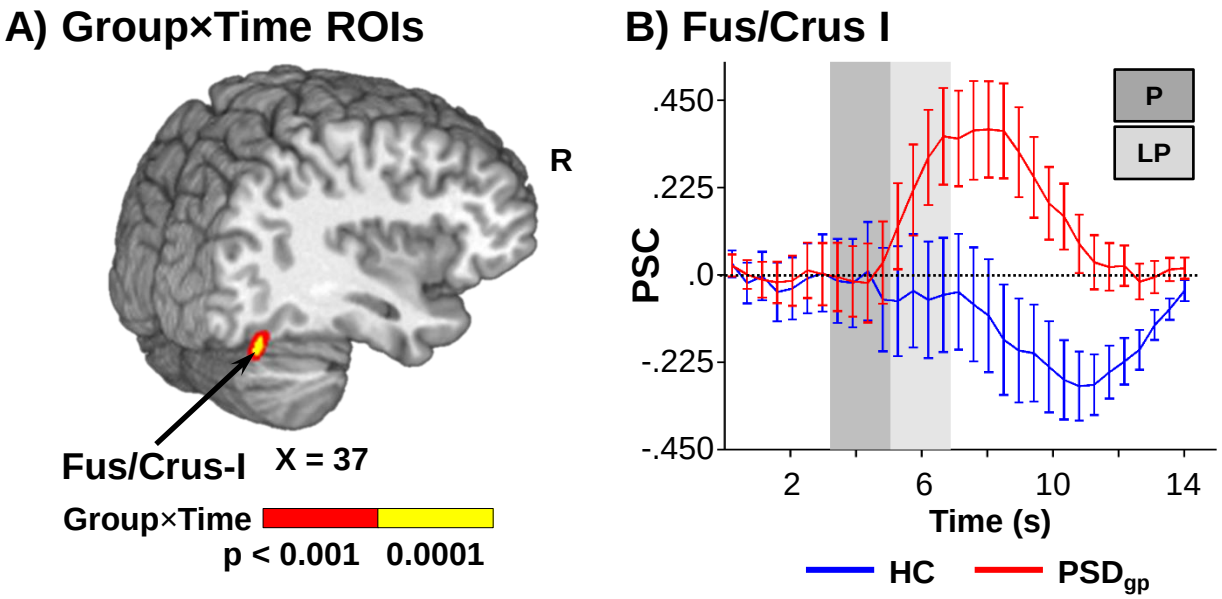

Supplemental Figure 2: Panel A displays significant Group×Time interaction within the right fusiform extending into crus I of the cerebellum (Fus/Crus-I) based on the Talairach atlas (X=sagittal slice location; R=right). Significance level is denoted by color (red: $p<0.001$; yellow: $p<0.0001$). Panel B depicts a line graph with standard error bars represent the percent signal change (PSC) from baseline for the average hemodynamic response averaged across reactive (AY) and proactive (BX) probe trials between HC (N=58; blue line) and PSD_{gp} (N=105; red line). Panel background shading designates Peak (P; dark grey) or Late-peak (LP; light grey) phases of the hemodynamic response.

Appendix 1 to Stephenson, D, El Shaikh, A, Shaff, N et al. Differing Functional Mechanisms Underlie Cognitive Control Deficits in Psychotic Spectrum Disorders. *J Psychiatry Neurosci* 2020.

DOI: 10.1503/jpn.190212

Online appendices are unedited and posted as supplied by the authors.

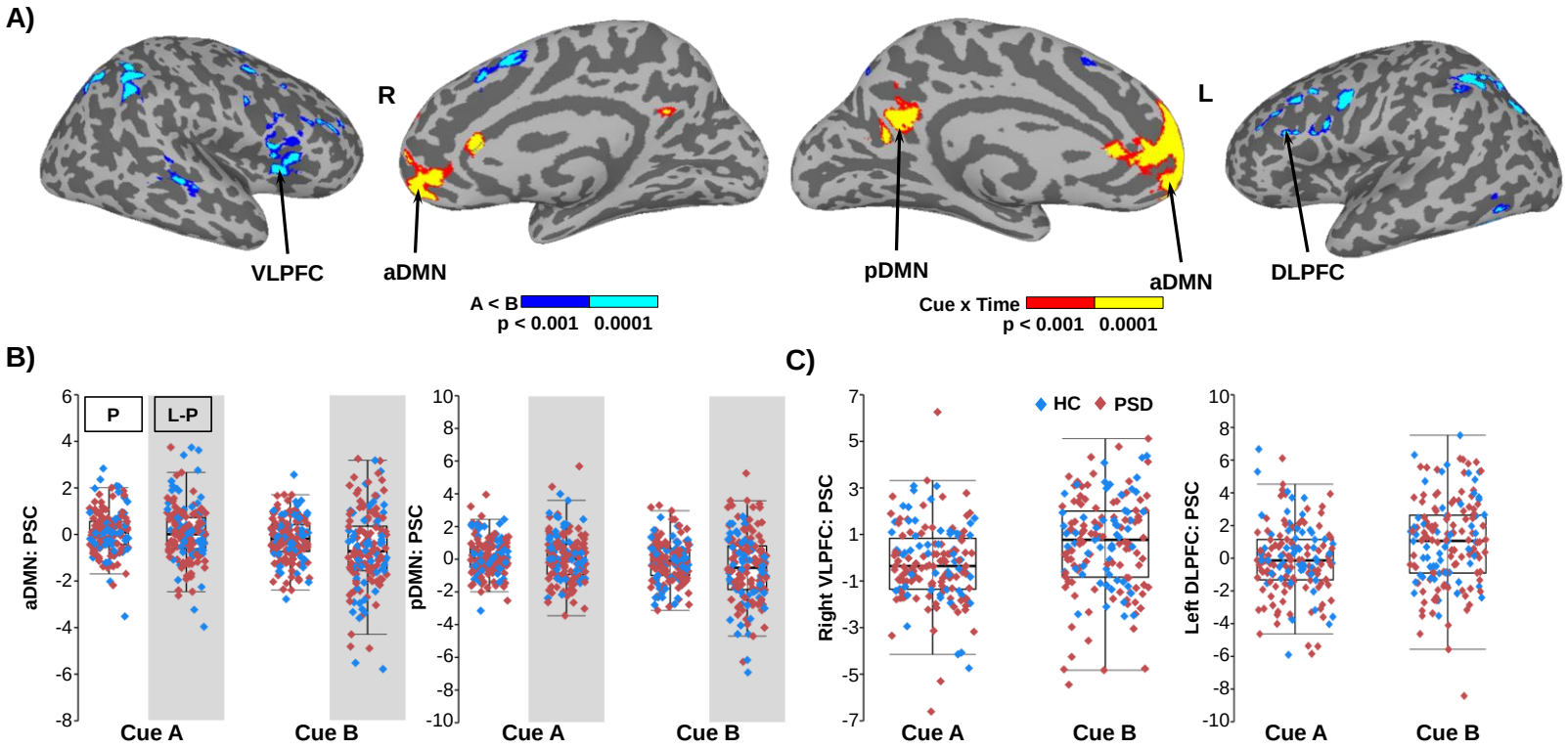

Supplemental Figure 3: Panel A contains inflated brain renders of the right (R) and left (L) hemispheres presenting significant clusters resulting from the main effect of Cue during a 2×2×2 [Group (PSD vs. HC) × Cue (A vs. B) × Time (Peak vs. Late-Peak)] ANCOVA. In the anterior (aDMN) and posterior (pDMN) default mode network, the main effect largely overlapped Cue×Time

Appendix 1 to Stephenson, D, El Shaikh, A, Shaff, N et al. Differing Functional Mechanisms Underlie Cognitive Control Deficits in Psychotic Spectrum Disorders. *J Psychiatry Neurosci* 2020.

DOI: 10.1503/jpn.190212

interaction results (Panel B). Additionally, a main effect of Cue was present in the right ventrolateral (VLPFC) and left dorsolateral (DLPFC) prefrontal cortex (Panel C). Significance level is denoted by color intensity for both the main effect alone (A<B; blue: $p<0.001$; cyan: $p<0.0001$) and Cue×Time interaction and main effect (A>B; red: $p<0.001$; yellow: $p<0.0001$). Box-and-scatterplots represent percent signal change (PSC) activity within these regions of interest, with shading in Panel B indicating Peak (white) versus Late-peak (grey) phases of the hemodynamic response of Cue×Time clusters. Healthy controls (HC; N=58; blue diamonds) and 'good' performing (≥56% accuracy on all conditions) patients with a psychotic spectrum disorder (PSD_{gp}; N=105; red diamonds) are presented in both panels for completeness.

Appendix 1 to Stephenson, D, El Shaikh, A, Shaff, N et al. Differing Functional Mechanisms Underlie Cognitive Control Deficits in Psychotic Spectrum Disorders. *J Psychiatry Neurosci* 2020.

DOI: 10.1503/jpn.190212

Online appendices are unedited and posted as supplied by the authors.

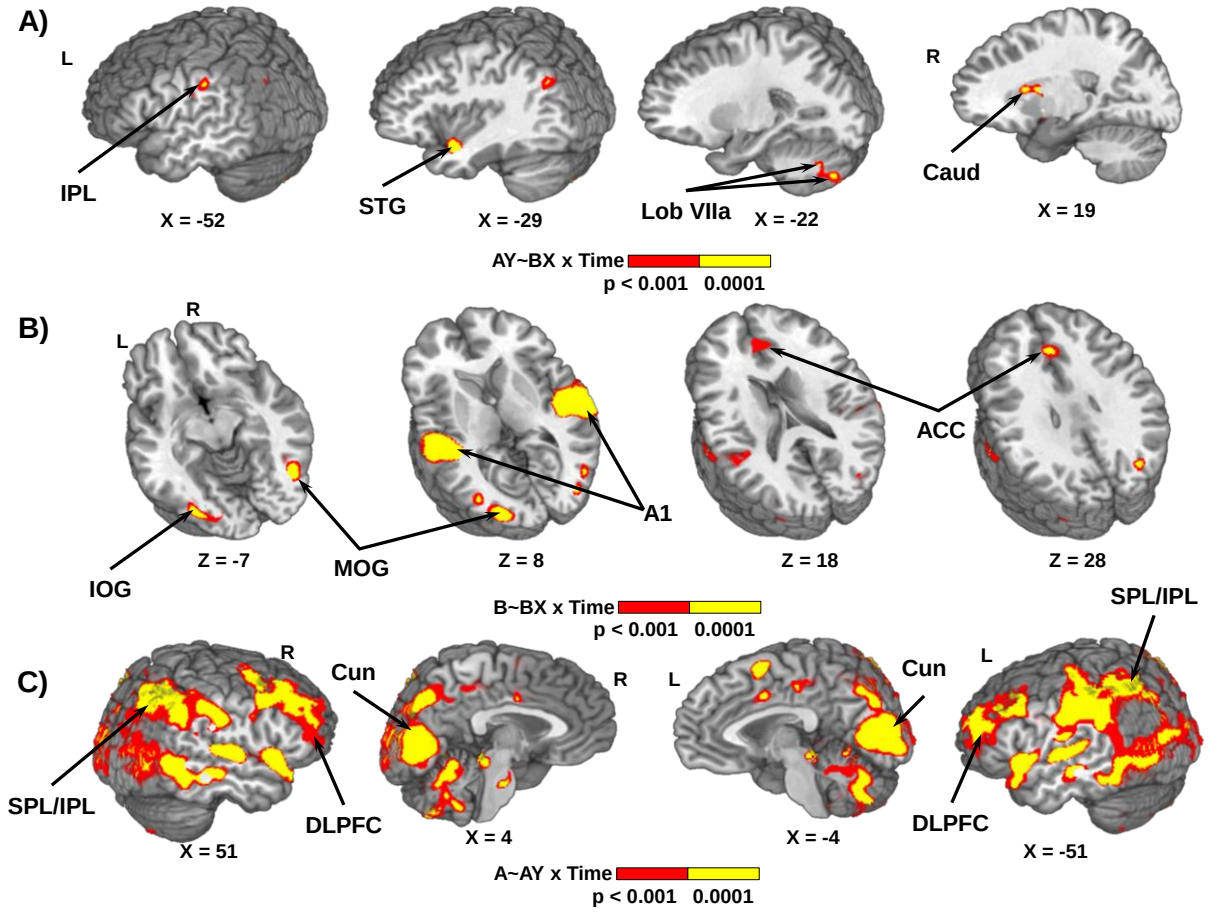

Supplemental Figure 4: This figure presents multiple brain renders in Talairach space (X=sagittal plane; Z=axial plane; left [L] and right [R] hemispheres) where there are significant clusters from the Condition×Time interaction in 2×2×2 [Group (PSD vs. HC) × Condition × Time (Peak vs. Late-Peak)] ANCOVA analyses. These include the Probe contrast (AY vs. BX; Panel A), as well as two Cue~Probe (B vs. BX, Panel B; A vs. AY, Panel C) contrasts. The significance of the omnibus test is denoted by color intensity (red: $p<0.001$; yellow: $p<0.0001$). Labelled regions include the dorsolateral prefrontal cortex (DLPFC), anterior cingulate cortex (ACC), superior temporal gyrus (STG), caudate (Caud), primary auditory cortex (A1), superior and inferior parietal lobe (SPL/IPL), middle occiptial gyrus (MOG), inferior occipital gyrus (IOG), cuneus (Cun), and lobule VIIa of the cerebellum (Lob VIIa).